Supporting Information for:

Water Oxidation Catalysis by Immobilization of the Dimanganese Complex $[Mn_2(\mu\text{-}O)_2Cl(\mu\text{-}O_2CCH_3)(bpy)_2(H_2O)](NO_3)_2$ onto Silica.

Evan M. W. Rumberger, Hyun S. Ahn, Alexis T. Bell, and T. Don Tilley**

Departments of Chemistry and Chemical Engineering, University of California at Berkeley, Berkeley California 94720, and Chemical Sciences Division, Lawrence Berkeley National Laboratory, 1 Cyclotron Road, Berkeley, California 94720 USA

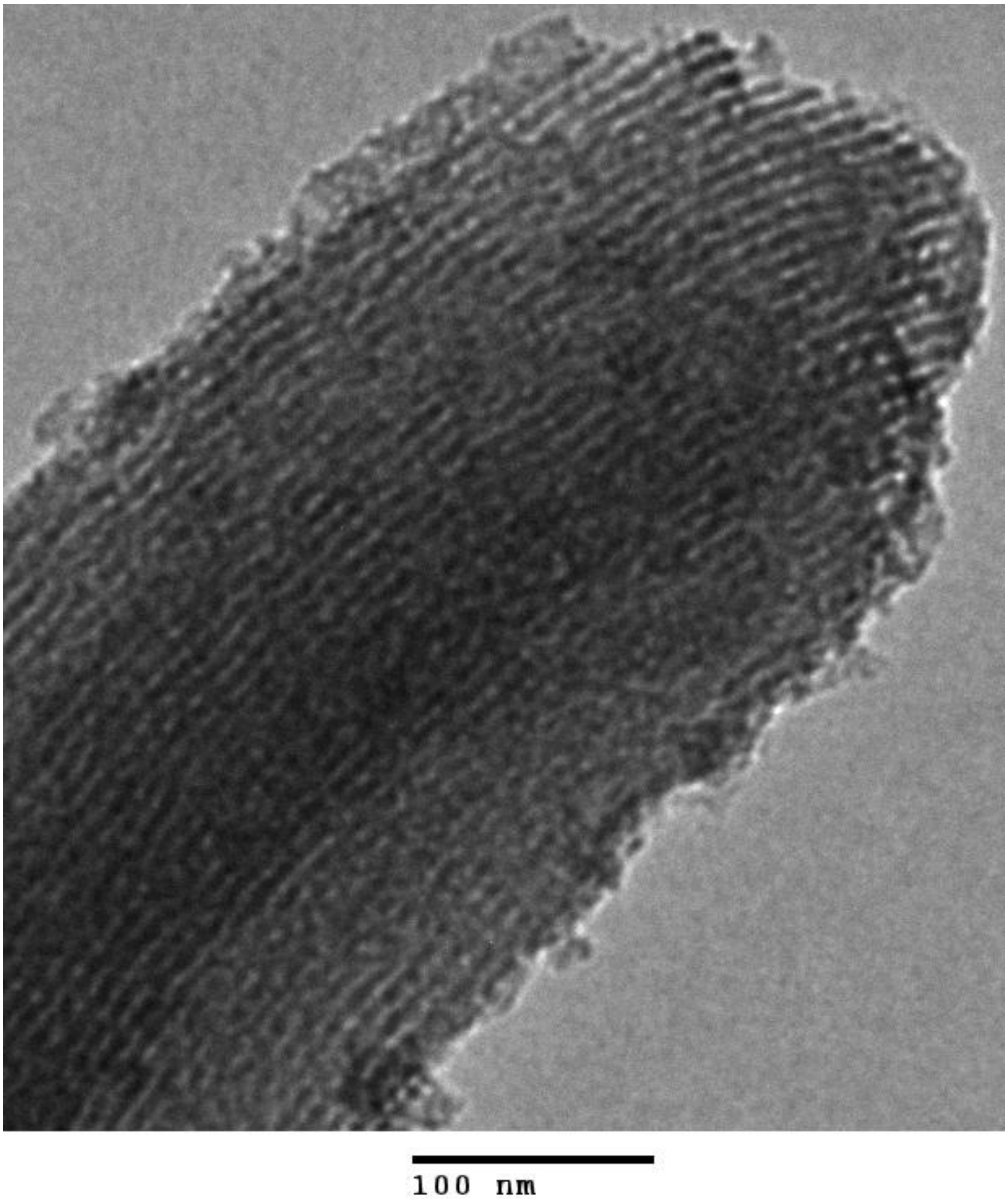

Figure S1. A typical TEM micrograph of the Mn_2-SBA15**(2)** material displaying no signs of Mn oxide nanoparticle formation (in the resolution of the instrument at ca. 10 nm).

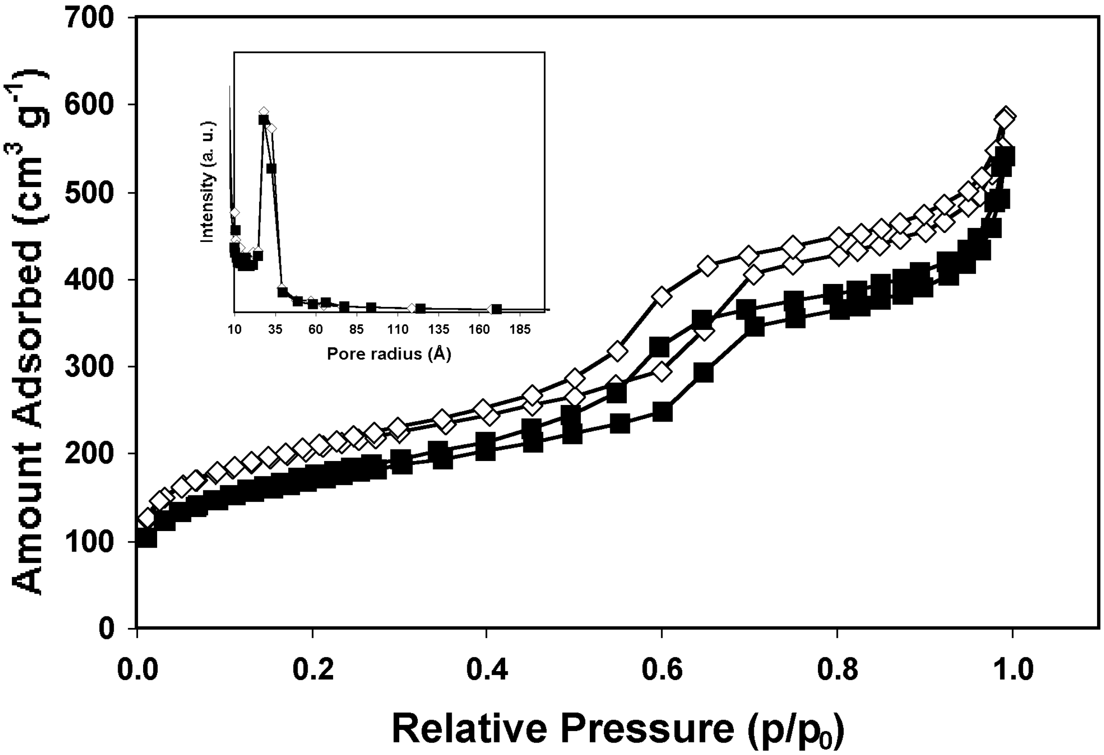

Figure S2. Nitrogen porosimetry adsorption / desorption isotherm with pore size distribution (insert) for the SBA15 (◊) and Mn_2-SBA15 (ν) materials.

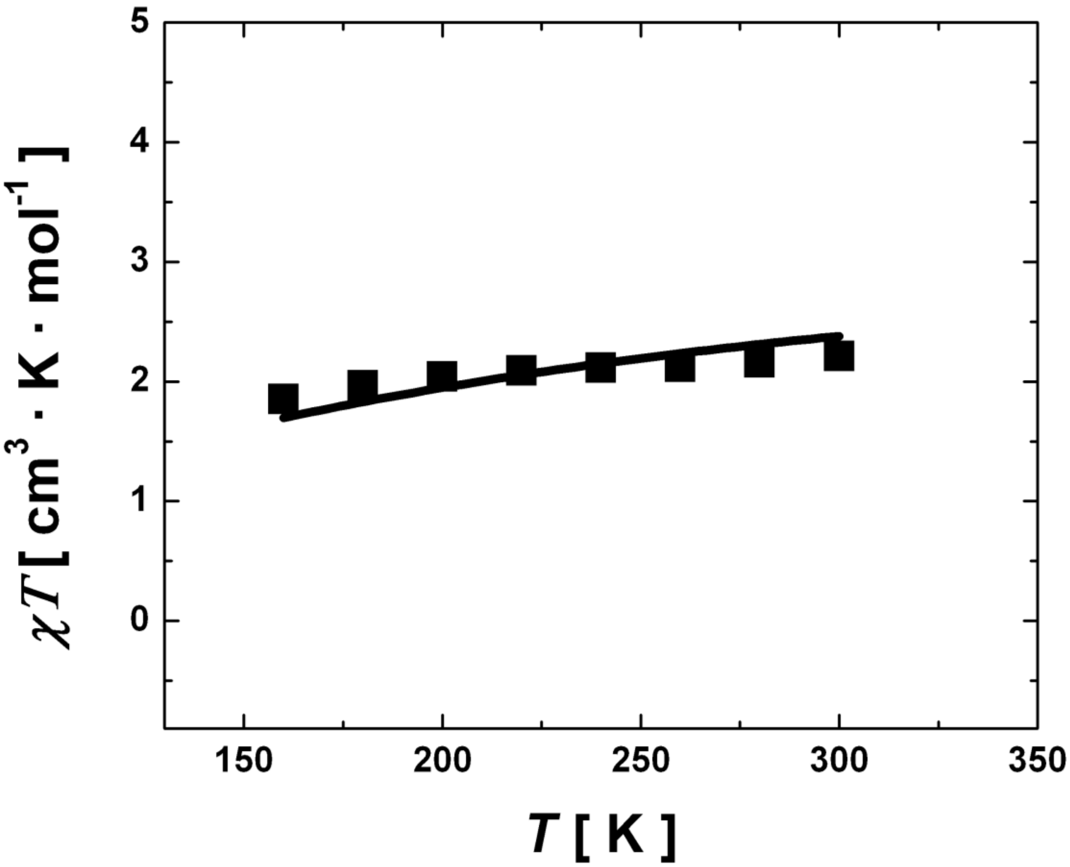

Figure S3. Plot of χT *vs.* T for the Mn_2SBA15 **(2)** material where χ is the molar susceptibility for the complex $[Mn_2O_2Cl(O_2CCH_3)(bpy)(H_2O)]^{2+}$ grafted on to the SBA15. The solid line represents a least-squares fit to the data with g = 2.0, J = -29 cm^{-1}; see the text for details.

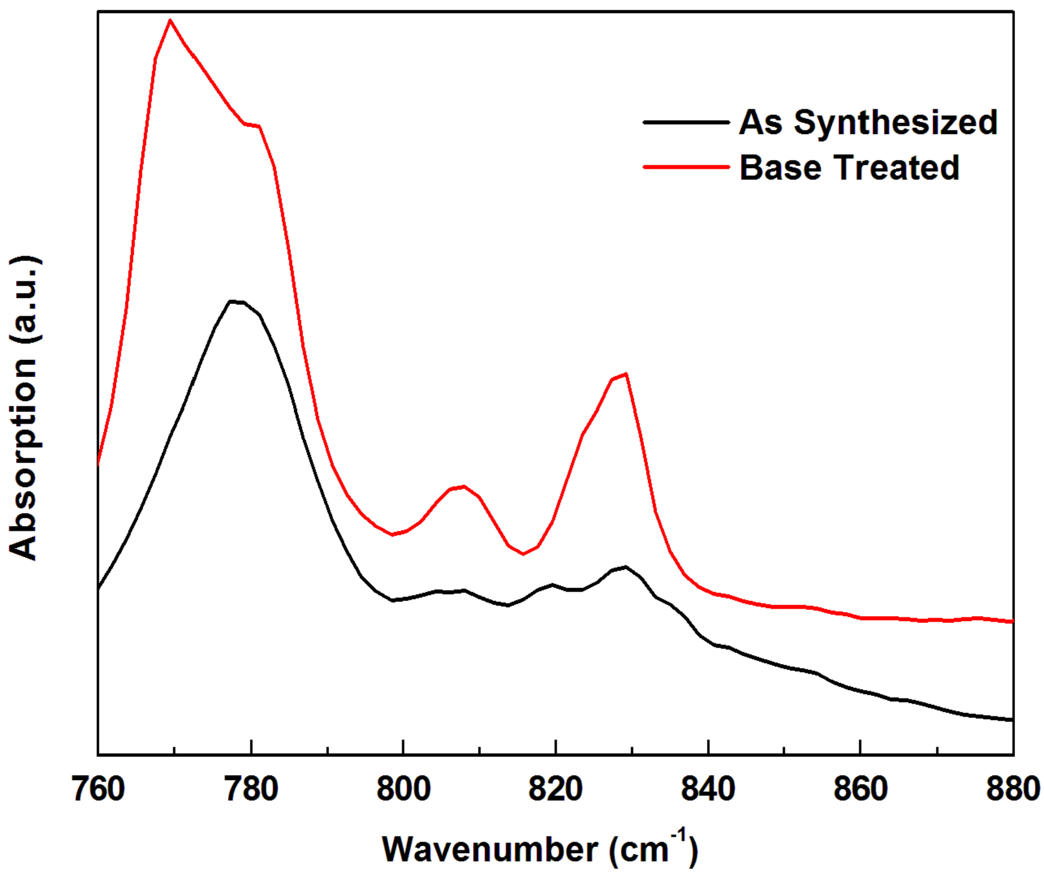

Figure S4. Diffuse reflectance FTIR spectrum of as synthesized **1** and that of **1** after base treatment.

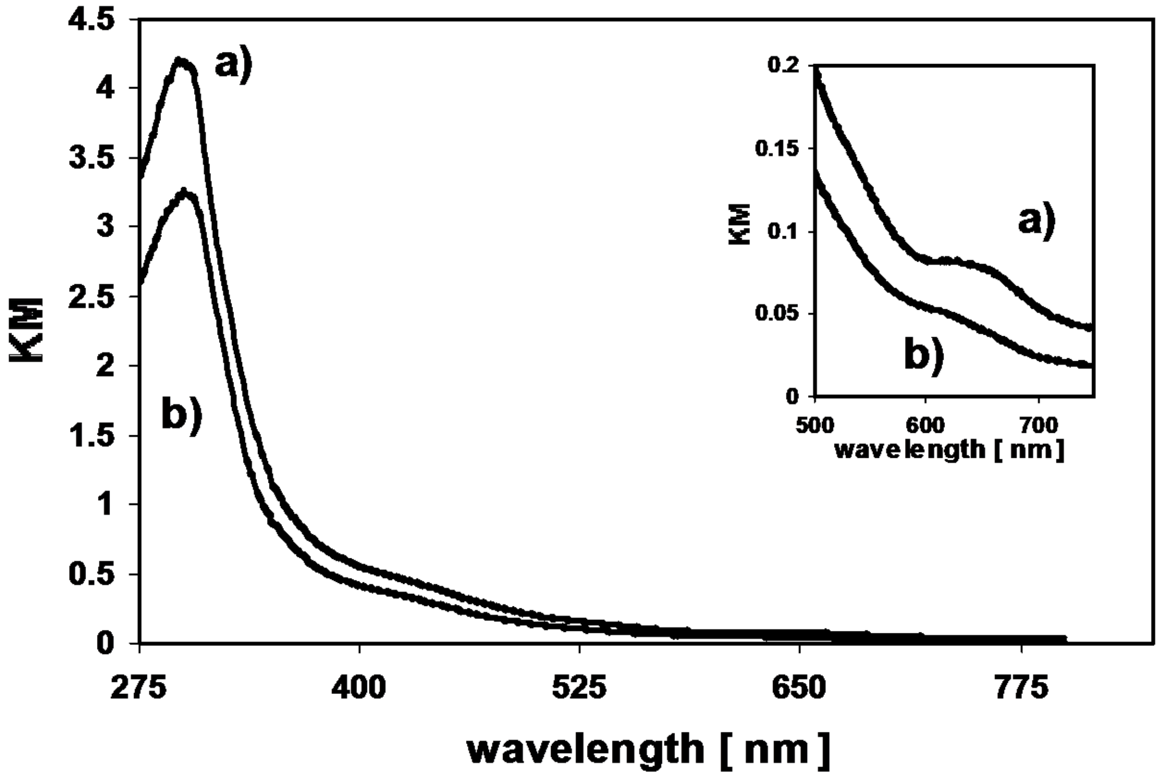

Figure S5. Diffuse reflectance UV-visible spectrum of the Mn_2-SBA15 **(2)** material before (spectrum a) and after receiving a water treatment (b). The inset is a magnification of the 500 - 750 nm region.

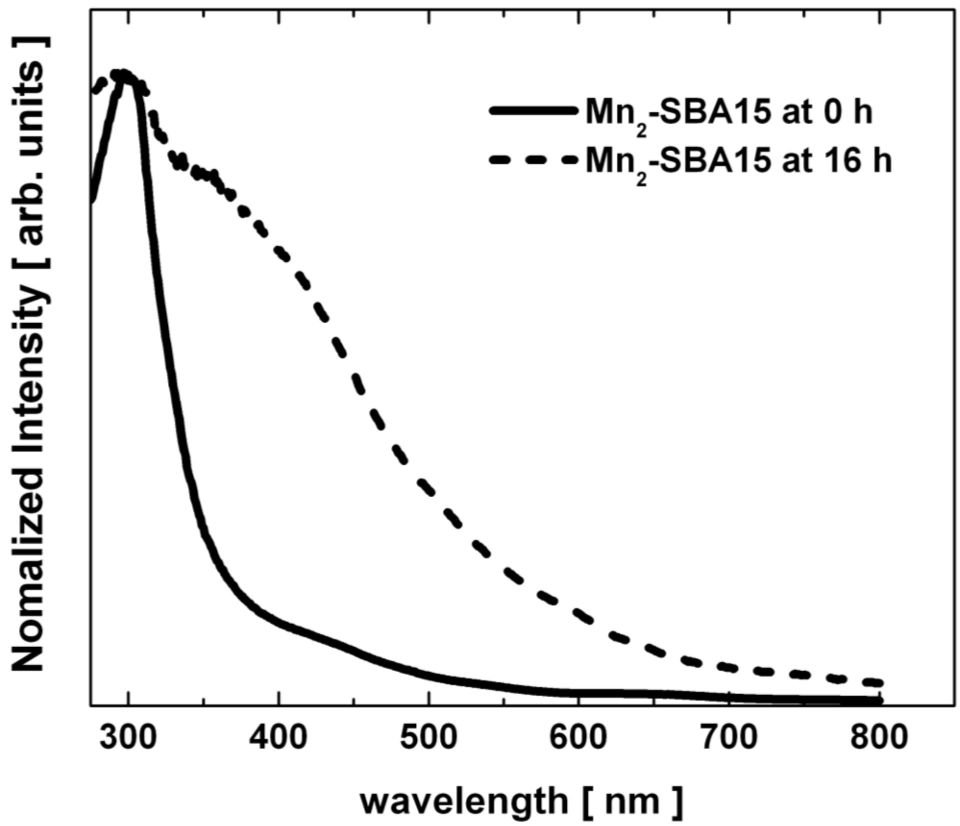

Figure S6. Diffuse reflectance UV-visible spectrum of the Mn_2-SBA15 **(2)** material before (solid line) and after being treated with a 200 mM solution of $(NH_4)_2Ce(NO_3)_6$.

Table S1. Parameters obtained from the analysis of the variable temperature magnetism data. Data for complex **1** are reproduced from reference 42.

	Complex **1**	Mn_2SBA15 **(2)**
g	1.97	2
J	-36.6 cm^{-1}	-29 cm^{-1}
χT @ 300K	2.23 cm^3 K mol^{-1}	2.2 cm^3 K mol^{-1}

Magnetic properties of supported $[Mn_2(\mu\text{-}O)_2Cl(\mu\text{-}O_2CCH_3)(H_2O)(bpy)_2]^{2+}$. The data for $\chi_M T$ versus temperature were least squares-fit to a theoretical model in order to ascertain the magnitude of the magnetic exchange interaction. The exchange interactions were represented with an isotropic spin Hamiltonian (eq. 1).

$$\hat{H} = -2J(\hat{S}_1 \hat{S}_2) \qquad (1)$$

Since

$$S_1 = S_2 \qquad (2)$$

for the Mn^{IV}_2 dinuclear complex **1**, there are only four possible total spin-states (S_T = 3,2,1,0). The eigenvalues of eq 2 were calculated using eq 3.

$$E(S_T) = -2S_T(S_T + 1) \qquad (3)$$

Theoretical susceptibilities were calculated from a least-squares fit of the experimental data to the Van Vleck equation (eq 5). The results of the analysis are listed in Table 1.

$$\chi_M = \frac{Ng^2\beta^2}{3kT} \frac{\sum [S_T(S_T+1)(2S_T+1)]e^{-E(S_T)/k_B T}}{\sum (2S_T+1)e^{-E(S_T)/k_b T}} \qquad (5)$$